Non-contact Local Conductivity Measurement of Metallic Nanowires Based on Semi-near-field Reflection of Microwave Atomic Force Microscopy

Bo Tong
Nagoya University
Takahiro Hirabayashi
Nagoya University
Yuhki Toku
Nagoya University
Yasuyuki Morita
Kumamoto University
Yang Ju (ju@mech.nagoya-u.ac.jp)
Nagoya University

Article

Keywords: atomic force microscopy, microwave, metallic nanowire, conductivity

Posted Date: January 14th, 2021

DOI: https://doi.org/10.21203/rs.3.rs-132530/v1

Version of Record: A version of this preprint was published at Applied Physics Express on May 11th, 2021. See the published version at https://doi.org/10.35848/1882-0786/abf444.

Non-contact Local Conductivity Measurement of Metallic Nanowires Based on Semi-near-field Reflection of Microwave Atomic Force Microscopy

*Bo Tong[1], Takahiro Hirabayashi[1], Yuhki Toku[1], Yasuyuki Morita[2], and Yang Ju[1]**

1. Department of Mechanical Science and Engineering, Nagoya University, Nagoya 464-8603, Japan

2. Faculty of Advanced Science and Technology, Kumamoto University, Kumamoto 860-8555, Japan

KEYWORDS: atomic force microscopy, microwave, metallic nanowire, conductivity

ABSTRACT: In this study, a non-contact and quantitative evaluation method was developed to measure the conductivity of metallic nanowires with a nanometer-scale spatial resolution. A coaxial probe was experimentally fabricated; using this probe, microwave images of the Al, Ag, and Cu nanowires and their topography images were simultaneously obtained via microwave atomic force microscopy (M-AFM) in the non-contact mode. A semi-near-field reflection model was established to describe the spatial distribution of a microwave between the tip of the probe and the sample. The local conductivities of metallic nanowires on the nanometer-scale can be

quantitatively evaluated in a single scan, using a metal strip substrate to calibrate the reflection signal.

Metallic nanowires have been promising functional materials for various applications, such as magnetic data storage media [1-3], giant magnetoresistance nanowires [4,5], metamaterials [6-8], thermoelectric power conversion [9,10], chemical or biological sensors [11,12], and transparent electrodes [13]. Conductivity is one of the most valuable properties for the application of metallic nanowires. Traditional evaluation method for metallic nanowires is based on the four-probe method [14-16], which is inefficient and may contaminate the sample because of the fabrication of tiny electrodes; to determine the cross-sectional area of the nanowires the observation with scanning electron microscopy (SEM) is necessary. Alternatively, atomic force microscopy (AFM) [17-19] has been demonstrated to be effective to characterize nanowires as a non-destructive metrology tool in the past several decades, due to its high spatial resolution and the free environmental vacuum degree. As a functionalized AFM, electrostatic force microcopy (EFM) was used to investigate the charge distribution on CdSe nanowires upon local illumination with a focused laser beam [20]. Moreover, the charge effect and surface potential variation of Cu, Cu_2O, and CuO nanowires based on the change of applied bias voltages were measured by EFM and Kelven probe force microcopy (KFM) [21]. I-V properties between an AFM tip and NiO nanowires were investigated by conductive AFM [22]. However, these techniques are difficult to measure the conductivity of nanowires based on their working mechanism. In addition, AFM has been combined with microwave system for the imaging and quantitative characterization of local surface electrical properties of nanomaterials and nanodevices. Scanning microwave microscopy

(SMM), has been developed to determine the dielectric constant of thin SiO_2 film and the resistivity of Si sample based on the capacitance and impedance measurements [23]. The relative permittivity of dielectric materials and sheet conductance of MoS_2 film on SiO/Si substrate have been measured by microwave impedance microscopy (MIM) [24]. However, there is few reports regarding to the measurement of nanowires, especially the conductivity measurement of metallic nanowires. On the other hand, in order to realize non-contact quantitative evaluation of local electrical properties, microwave AFM (M-AFM) composed of a w-band microwave system and AFM has been developed, and a slit probe which can propagate and emit a microwave by itself has been designed and fabricated [25, 26]. This probe helps to realize simultaneous scanning of topography images and microwave reflection measurement; the quantitative evaluation of the conductivities of metallic films in non-contact mode has been achieved [27, 28].

Nevertheless, it is still a challenge to quantitatively measure the conductivity of metallic nanowires. Different from the scan on a flat surface, the measurement of nanowires is also affected by its surface shape because the tip aperture of the probe is comparable with the diameter of the nanowires. Moreover, the change of local resistance between different metallic nanowires is too small. To the best of our knowledge, so far there is still not any technology which can measure the conductivity of individual metallic nanowires in-situ. In this study, the quantitative determination of the conductivity of metallic nanowires using M-AFM was firstly demonstrated. To increase the measurement sensitivity thereby identify the difference of the reflection coefficients of different metallic nanowires, a new M-AFM probe, of which the tip was designed as coaxial structure, was fabricated. To solve the problem that the reflected signal also depends on the diameter of the nanowires, a theoretical model based on semi-near-field model was established to describe the spatial distribution of the electric field between the tip and the sample. The distance between the

tip of the probe and the sample impacting the intensity of the microwave applied on the sample was also considered. The scanned microwave images of Al, Ag, and Cu nanowires on a metal strip substrate, which can be used to calibrate the reflection signal, were measured using the coaxial probe. According to the theoretical model, the conductivities of these nanowires were determined quantitatively from the reflected signal measured by M-AFM.

Fig. 1(a) and 1(b) show the schematics of the coaxial M-AFM probe. In this experiment, the tip of the probe was designed based on both the AFM probe and the coaxial transmission line. The SEM images are shown in Fig. 1(c) and 1(d). By photolithography and wet etching, the cantilever and tip of the probe were fabricated from a piece of non-doped GaAs wafer (see Fig. 1(c)). A pyramid hole was dug on the reverse surface by focus ion beam (FIB) etching right at the position of the tip (see Fig. 1(b) and 1(d)). The alignment was performed based on the position from the end of the cantilever. To fabricate the waveguide that can confine the microwave inside the probe, both the top and bottom surfaces of the probe were coated with Au films by electron beam evaporation. The Au films on the tip and in the pyramid-hole serve as the outer and inner conductors of the coaxial structure, respectively (see Fig. 1(a), 1(b), and 1(c)). Finally, using FIB etching, a small hole was fabricated at the end of the tip through the Au film, which serves as the aperture to emit microwave (see Fig. 1(b) and inset in Fig. 1(c)). The aperture size of the tip is 250 nm approximately, according to the SEM image. It should be mentioned that it is better to fabricate the aperture of the tip as small as possible in order to avoid the microwave response being affected by the topography of the nanomaterials.

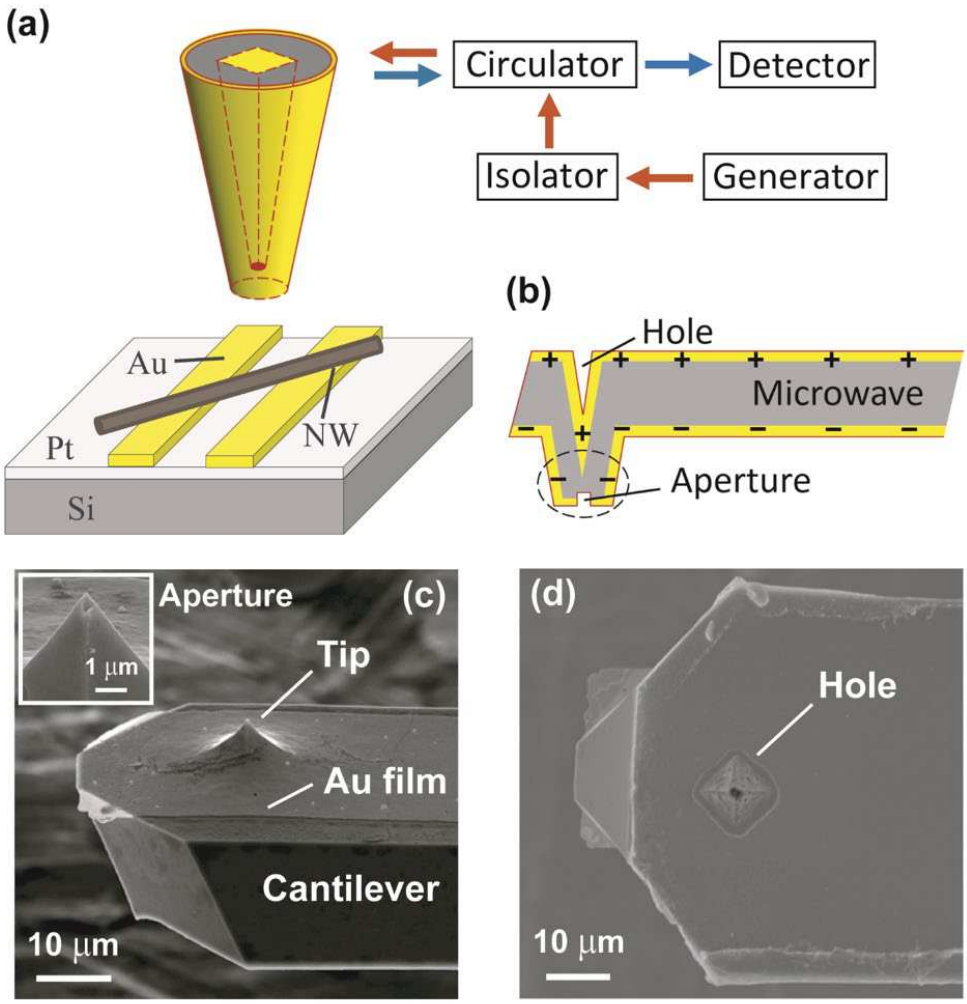

Figure 1. (a) Schematic of the tip of the coaxial M-AFM probe, calibration substrate, and the microwave system. The red arrows indicate the incident signal, and the blue arrows represent the reflected signal. (b) Schematic profile of the coaxial M-AFM probe. The gray and golden parts represent the GaAs and Au films, respectively. The tip in (a) corresponds to the part marked by the dashed circle in (b). SEM images of the (c) tip side and (d) back side of a coaxial M-AFM probe. The inset in figure (c) depicts the aperture fabricated on the tip.

In the quantitative evaluation experiment, Al, Ag, and Cu nanowires with diameters of 660 nm,

240 nm, and 720 nm were prepared, respectively. Each sample was scanned in non-contact mode on a Pt substrate with Au strips (see Fig. 1(a)), which can be used for the calibration of the reflected signal. Both the width and interval of the strips were 5 μm. The scanning speed was 3 μm/s, and the scanning area was 10×10 μm^2 for the Ag nanowire and 20×20 μm^2 for the Al and Cu nanowires, based on their sizes. A 94 GHz microwave signal having 10 dBm source power was applied to the probe. The dimensions of the cantilever and the support part of the probe were designed to have a characteristic impedance of 50 Ω at the working frequency of 94 GHz [25]. As the probe tip has a coaxial structure, the emitted microwave is in TEM mode having electric field in the radial direction and magnetic field in the circumferential direction. After being reflected by the sample, the microwave signal is received by a detector (see Fig. 1(a)). In this study, the microwave detector works in a small signal range and provides a direct-current output voltage proportional to the square of the amplitude of the electric field of the inputted microwave, which can be written as [28]

$$V = k_0 \left| E_2 \right|^2 + b_0 . \tag{1}$$

Here, E_2 is the intensity of the reflected microwave, and k_0 and b_0 are the performance parameters of the square-law detector. The measurement was conducted in air, and the temperature and relative humidity of the environment was 20.0 ℃ and 50%, respectively.

Considering that the wavelength of the microwave (~ 3 mm) is much longer than the tip-sample distance (~ 5 nm), the measurement result should be analyzed by a near-field model to improve the accuracy. At every instant the electric field of the incident and reflected microwave can be approximated as quasi-static fields produced by the original charge on the probe and the polarization charge on the sample. According to the conclusion of electrostatics, the polarization charge can be represented by image charge for simplification [29]. When the probe is located over

the Au strips or the Pt substrate, which can be regarded as an infinite and isotropic plane within the size of the tip of the probe, the image charge is mirror-symmetrical to its original charge on the probe. Therefore, if the charge on the tip is considered to mainly exist on the outer surface of the inner conductor and on the inner surface of the outer conductor, the image charge should exhibit an identical double-tube-like distribution, as shown in Fig. 2(a). When the probe moves over a metallic nanowire sample whose diameter is $2r$, since only the local part of the nanowire under the tip is evaluated, the sample surface can be approximated as a spherical surface with the same radius of r, and thus, the image charges form a double-trumpet-like distribution, as shown in Fig. 2(b). In this case, if a single point charge q_1 is located above this surface at a distance z_1, the image charge q_2 and its position can be determined as

$$q_2 = -\frac{r}{z_1 + r} q_1, \tag{2}$$

and

$$z_2 = \frac{z_1 r}{z_1 + r}, \tag{3}$$

respectively. Here, z_2 is the distance of the image charge q_2 from the surface of the sphere.

However, it should be pointed out that this thorough near-field model describes only the distribution of the electric field which is independent of the conductivity of the sample. In order to describe the conductivity dependence of the reflected wave, the reflection coefficient Γ is combined with this model to establish a semi-near-field model. On the surface of the substrate or sample, the reflected wave E_2 and the incident wave E_1 should obey the relation as [30]

$$\Gamma = \frac{E_2}{E_1} = \frac{\eta - \eta_0}{\eta + \eta_0}, \tag{4}$$

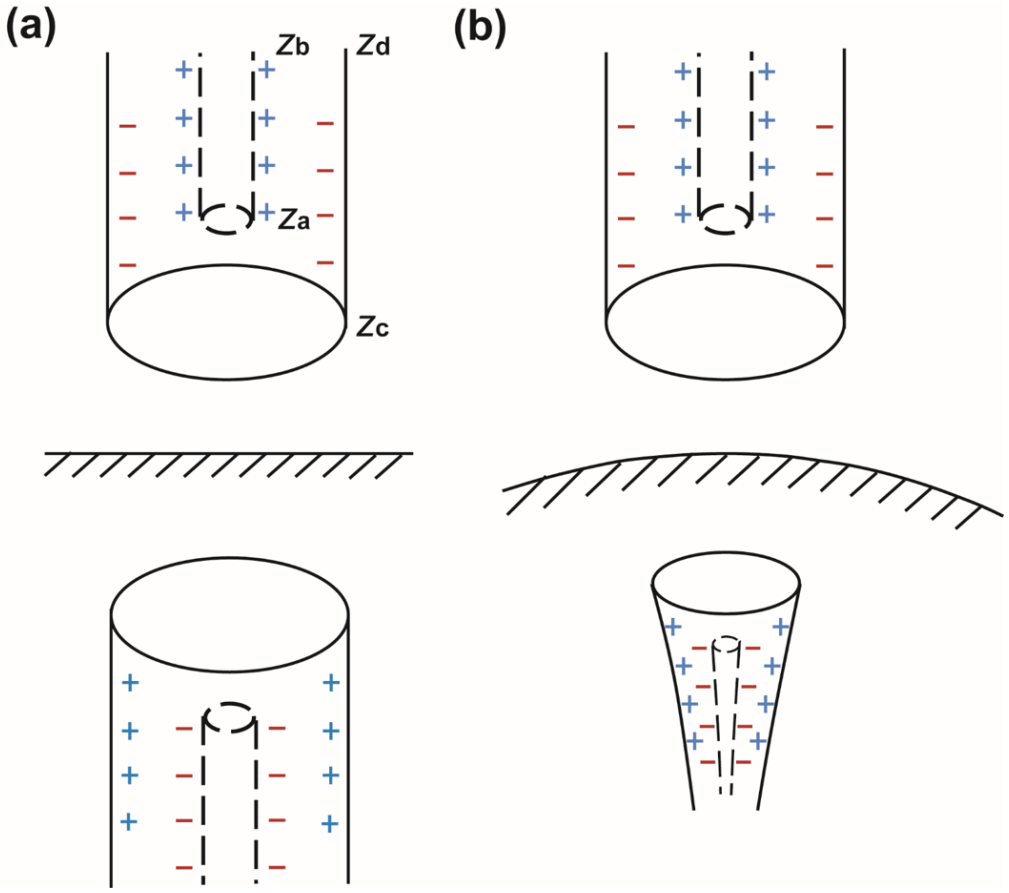

Figure 2. Schematic of image charge when the coaxial probe is over (a) a plane surface and (b) a spherical surface.

where η and η_0 are the impedance of the material and free space, respectively. They can be represented as $\eta = \sqrt{\mu_0\omega/(\varepsilon\omega - j\sigma)}$ and $\eta_0 = \sqrt{\mu_0/\varepsilon_0}$, where j, μ_0, ε_0, ε, σ, and ω are the imaginary unit, permeability and permittivity of free space, permittivity of the sample, conductivity of the sample, and frequency of the microwave, respectively. Combining Eq. (2) which describes the spatial distribution of the reflected wave and Eq. (4) which contains the conductivity of the material, the image charge in the semi-near-field model can be represented as

$$q_2 = -\frac{r}{z_1 + r}|\Gamma| q_1 . \tag{5}$$

Therefore, considering q_1 as a charge element on the tip, the reflected microwave can be calculated as the electric field integral of q_2, using the Coulomb law. If z_{i1}, ρ_{i1} and w_{i1} express the vertical distance of a charge element on the inner conductor from a nanowire surface, the linear charge density along the inner conductor and the diameter of the inner conductor, respectively, the corresponding quantities of its image charge element in the nanowire sample, which are represented as z_{i2}, ρ_{i2} and w_{i2}, can be calculated as

$$z_{i2} = r - \frac{r^2\left(r + z_{i1}\right)}{\left(w_{i1}/2\right)^2 + \left(r + z_{i1}\right)^2}, \tag{6}$$

$$\rho_{i2} = \frac{r}{\sqrt{\left(w_{i1}/2\right)^2 + \left(r + z_{i1}\right)^2}}\rho_{i1}, \tag{7}$$

and

$$w_{i2} = \frac{r^2}{\left(w_{i1}/2\right)^2 + \left(r + z_{i1}\right)^2}w_{i1}. \tag{8}$$

The corresponding quantities of the outer conductor z_{o2}, ρ_{o2} and w_{o2} also have the same relationship with z_{o1}, ρ_{o1} and w_{o1} as long as the subscript i in Eqs. (6), (7) and (8) is replaced with o. Therefore, the reflected wave from a nanowire sample calculated by Coulomb law has the following form:

$$E_2 = \frac{|\Gamma|}{4\pi\varepsilon_0}\left\{\int_{z_a}^{z_b}\frac{\rho_{i2}\left(z_0 + z_{i2}\right)\mathrm{d}z_{i1}}{\left[\frac{w_{i2}^2}{4} + \left(z_0 + z_{i2}\right)^2\right]^{3/2}} + \int_{z_c}^{z_d}\frac{\rho_{o2}\left(z_0 + z_{o2}\right)\mathrm{d}z_{o1}}{\left[\frac{w_{o2}^2}{4} + \left(z_0 + z_{o2}\right)^2\right]^{3/2}}\right\}. \tag{9}$$

Here, z_0 is the vertical distance of the apex of the tip from the substrate surface. z_a, z_b, z_c, and z_d represent the boundary region from the apex of the inner conductor and the outer conductor, as

shown in Fig. 2(a). The calculated electric field is the reflected wave at the center of the tip. This field represents the signal that is received and further propagated through the probe and waveguide until arriving at the diode detector. Although z_0 is not constant in the experiment because of the vibration of the tip working in non-contact mode, it can be considered as a constant by using its average value, as the measured signal only corresponds to the microwave signal obtained at the average position of the tip vibration. Based on the conservation of charge, the charge density on the boundary area of the tip should follow

$$\rho_{i1}\left(z_b - z_a\right) = -\rho_{o1}\left(z_d - z_c\right) = q_0 , \tag{10}$$

where q_0 is the total charge on the tip. In quantitative calculation, the depth of the boundary area is considered to be the same as the width of the aperture, which implies that $z_d - z_c = w_o$. For the reflection from the substrate and Au strips, the reflected microwave can be easily obtained using Eqs. (6), (7), (8) and (9), for $r = \infty$.

Finally, by substituting Eq. (9) into Eq. (1), the relation between the output voltage of the detector and reflection coefficient of the sample can be expressed as

$$V = k_1 k_2 \left|\Gamma\right|^2 + b_0 . \tag{11}$$

Here, k_1 represents a performance parameter of M-AFM which is determined not only by k_0, but also by the attenuation of microwave propagation and the charge on the probe tip. Moreover, k_1 and b_0 are constant parameters that need to be calibrated experimentally. k_2, however, represents the near-field effect on the spatial distribution of the electric field and can be calculated according to Eq. (9) as

$$k_2 = \left\{ \int_{z_a}^{z_b} \frac{r}{\sqrt{\frac{w_{i1}^2}{4} + \left(r + z_{i1}\right)^2}} \frac{\left(z_0 + z_{i2}\right)/\left(z_b - z_a\right) \mathrm{d}z_{i1}}{\left[\frac{w_{i2}^2}{4} + \left(z_0 + z_{i2}\right)^2\right]^{3/2}} \right.$$

$$\left. - \int_{z_c}^{z_d} \frac{r}{\sqrt{\frac{w_{o1}^2}{4} + \left(r + z_{o1}\right)^2}} \frac{\left(z_0 + z_{o2}\right)/\left(z_d - z_c\right) \mathrm{d}z_{o1}}{\left[\frac{w_{o2}^2}{4} + \left(z_0 + z_{o2}\right)^2\right]^{3/2}} \right\}^2, \tag{12}$$

If the substrate and strip contain two reference materials with known conductivities, using Eq. (11) the parameter k_1 and b_0 can be determined. Then, $|\Gamma|^2$ of the nanowire samples can be evaluated based on the measured voltage, and the conductivity of the materials can be obtained from Eq. (4).

The scanning topography image and microwave image of three metallic nanowire samples, Al, Ag, and Cu, were measured simultaneously by M-AFM, as shown in Fig. 3. It is observed that the microwave image corresponds to the topography image, which confirms that this coaxial tip can emit a microwave. The average detector output voltages along the center line of each strip or nanowire were extracted as the reflected voltage signal of the microwave, thereby avoiding the measurement error caused by the resolution near the boundary. The reflected voltage signal versus the standard conductivity of each material is shown in Fig. 4(a), 4(b), and 4(c). Here, as the thicknesses of the metal film and strips on the substrate are 300 nm and the diameters of all the nanowires are more than 200 nm, the size effect of conductivity is not considered. The standard conductivities are referred from the values of corresponding bulk materials [31, 32]. As the microwave signal strongly depends on the tip to sample distance, the error bar of the average reflected voltage signal mainly originates from a small change in the standoff distance in different scans. One abnormal phenomenon to be noted is the discordance of the Al nanowire. According

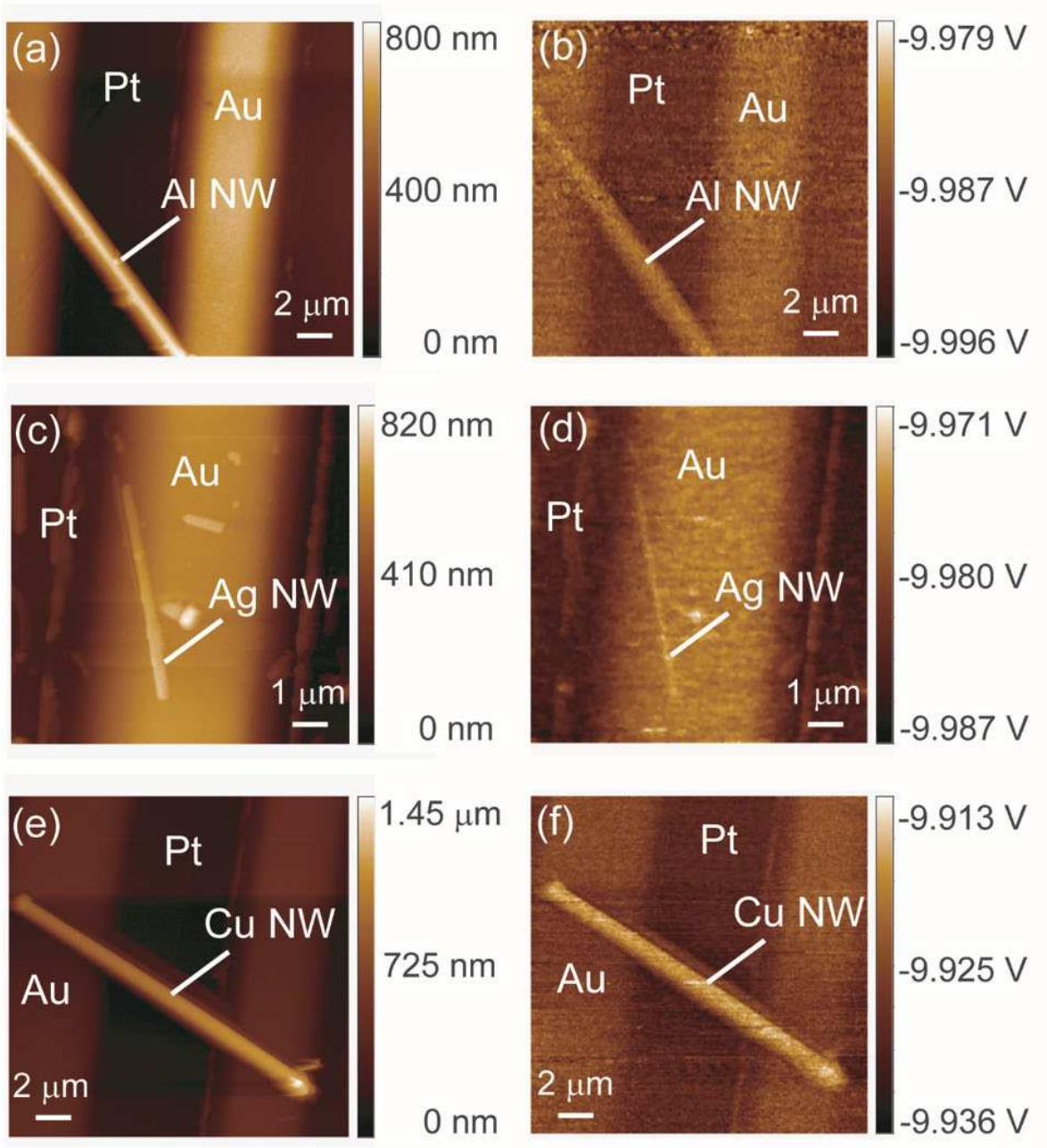

Figure 3. Scanning topography image (left) and microwave signal image (right) of the Al (a, b), Ag (c, d), and Cu (e, f) nanowires on the Pt substrate with Au strips.

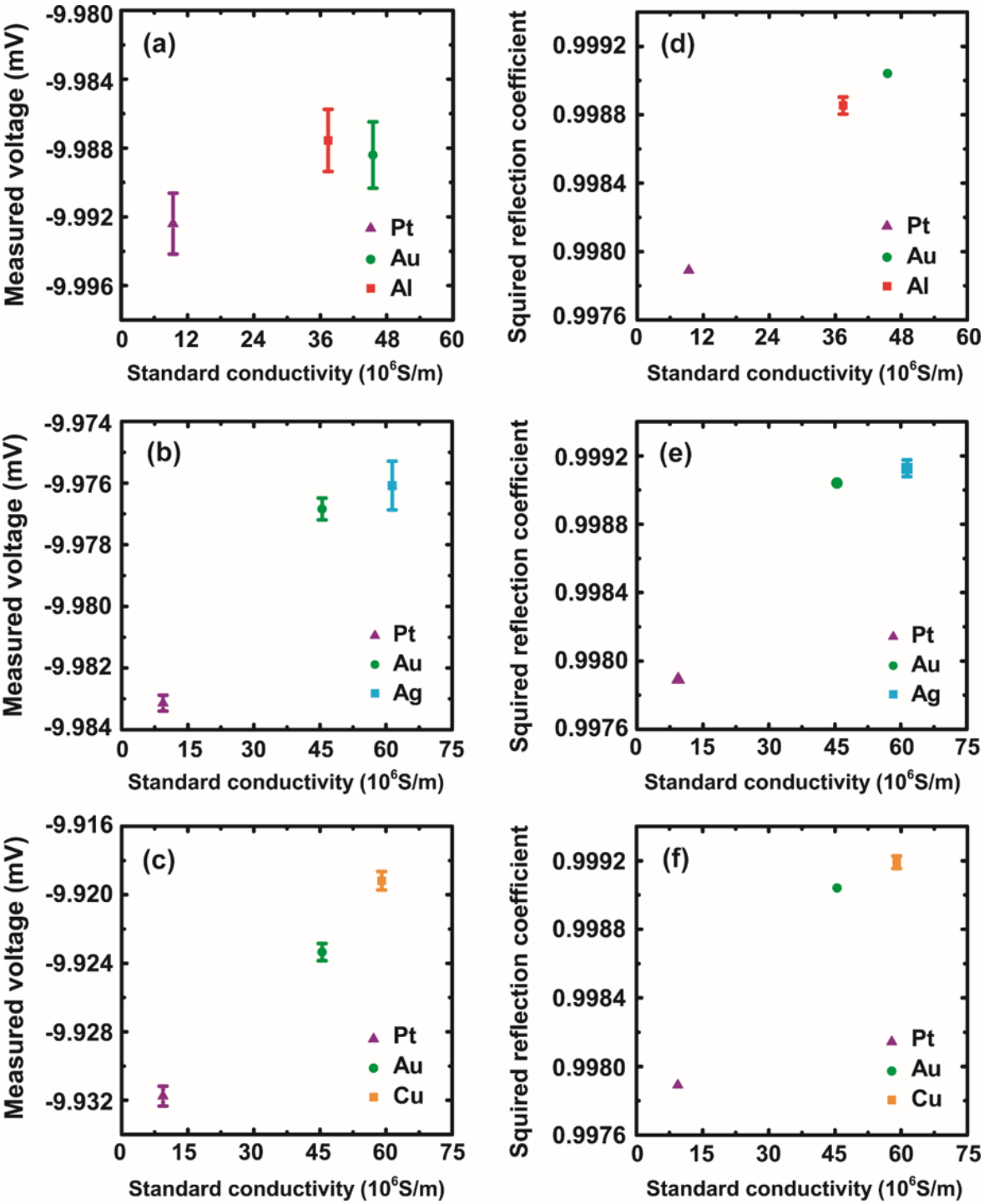

Figure 4. Reflected voltage signals of the (a) Al, (b) Ag, and (c) Cu nanowire samples with the signals of the Pt substrate and Au strip in each measurement, with respect to their standard conductivities. Evaluated results of the square of the surface reflection coefficient $|\Gamma|^2$ of the (d) Al, (e) Ag, and (f) Cu nanowire samples with respect to their standard conductivities compared

with the theoretical $|\Gamma|^2$ values of Au and Pt.

to Eqs. (4) and (11), the reflected voltage signal depends on the conductivity of the material monotonously. However, although the true conductivity of Al is higher than that of Pt and lower than that of Au, the measured reflected voltage signal of the Al nanowire is higher than that of both Pt substrate and Au strip, as shown in Fig. 4(a). This is because the curved surface of the nanowire generates a trumpet-like image charge that is more concentrated under the tip, as shown in Fig. 2(b), and thus generates a stronger reflected wave than the plane surface of the strip. The evaluation of the different near-field distribution of the microwave on the plane surface and curved surface results in the difference of k_2 in Eqs. (11). According to Eq. (12), k_2 of the substrate and the strip was calculated to be 1.56070×10^{10} m^{-2}, and k_2 of the three nanowire samples were 1.56138×10^{10} m^{-2} for Al, 1.56083×10^{10} m^{-2} for Ag, and 1.56133×10^{10} m^{-2} for Cu, respectively, according to their different diameters. Here, w_{i1} was determined to be 5 nm according to the resolution limit of our FIB etching; w_{o1} was determined to be 250 nm according to the SEM image of the tip; z_0 was determined to be 5 nm according to the M-AFM standoff distance while scanning.

Using the standard conductivities and reflected voltage signal of the Pt substrate and Au strip, the two undetermined parameters k_1 and b_0 of each measurement can be calibrated using Eq. (11). Subsequently, the square of the reflection coefficient on the surface of Al, Ag, and Cu nanowires, which is represented as $|\Gamma|^2$, can be calculated from the measured voltage signal by the same equation. The results of nanowires, Pt substrate, and Au strip versus their standard conductivities are shown in Fig. 4 (d), 4(e), and 4(f), respectively. From these results, it is noted that $|\Gamma|^2$ on the surface of the sample, substrate or strip depends on the conductivity of the materials monotonously. Therefore, the near-field model of the substrate and nanowire is demonstrated to be appropriate

for the description of the electric field distribution of M-AFM probe. Further, the conductivity of the three nanowire samples can be calculated from their surface reflection coefficient by Eq. (4). As shown in Fig. 5, the deviation of the evaluated conductivities from the standard values for Al, Ag, and Cu nanowires are 14.21%, 10.26%, and 8.57%, respectively. The deviations are due to both theoretical and experimental reasons. Firstly, the interaction caused by the near-field microwave was calculated based on a quasi-static charge model. As a part of the electrical interaction between the charges on the tip and the sample, the reflected wave also impacts the charge distribution on the tip, which was omitted in this model for simplification. Secondly, the experimental reason is that the shape of the fabricated tip is not as regular and symmetric as designed because of the resolution limit of FIB etching, which also impacts the true distribution of the microwave.

In this study, a coaxial probe was designed and fabricated. Using this probe, the topography image and reflected microwave image of the Al, Ag, and Cu nanowires were simultaneously obtained under the non-contact mode of M-AFM. The measurement was conducted on a Pt substrate with Au strips, for the calibration of the reflected signal. A semi-near-field model based on the image charge method and the reflection coefficient was established to describe the spatial distribution and conductivity dependence of a microwave between the tip and the sample. This is essential for non-contact quantitative measurements and may overcome the impact of nanowire diameter on measurement results. Through the calibration technique and expressions in this theoretical model, for the first time, the non-contact local conductivity evaluation of metallic nanowires was quantitatively achieved in a single scan. This indicates that M-AFM is a promising in-situ method for the characterization of one-dimensional nanomaterials.

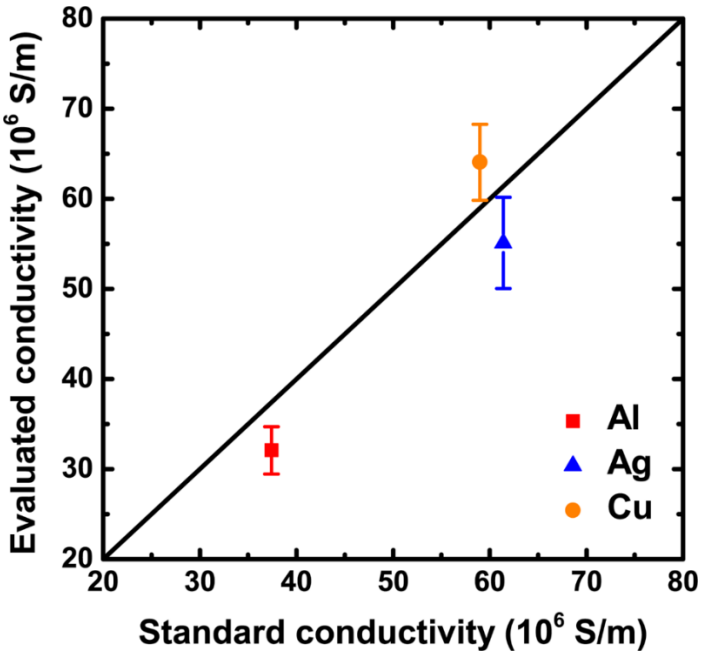

Figure 5. Evaluated conductivities of the Al, Ag, and Cu nanowires compared with their standard values.

AUTHOR INFORMATION

Corresponding Author

Yang Ju - Department of Mechanical Science and Engineering, Nagoya University, Nagoya 464-8603, Japan; E-mail: ju@mech.nagoya-u.ac.jp

Authors

Bo Tong - Department of Mechanical Science and Engineering, Nagoya University, Nagoya 464-8603, Japan

Takahiro Hirabayashi - Department of Mechanical Science and Engineering, Nagoya University, Nagoya 464-8603, Japan

Yuhki Toku - Department of Mechanical Science and Engineering, Nagoya University, Nagoya 464-8603, Japan

Yasuyuki Morita - Faculty of Advanced Science and Technology, Kumamoto University, Kumamoto 860-8555, Japan

Author Contributions

B. Tong established the model, performed the analysis and wrote the draft of the manuscript. T. Hirabayashi performed the probe fabrication and measurement experiments. Y. Toku, and Y. Morita assisted in the preparation of the experiment, analysis and the manuscript, and critically reviewed the manuscript. Y. Ju found and designed the study, improved and approved the manuscript.

ACKNOWLEDGMENT

This work was supported by the Japan Society for the Promotion of Science under Grants-in-Aid for Scientific Research (S) 17H06146.

ABBREVIATIONS

AFM, atomic force microscopy; M-AFM, microwave atomic force microscopy; SEM, scanning electron microscopy; TEM, transverse electromagnetic; FIB, focus ion beam

REFERENCES

1. Thurn-Albrecht, T.; Schotter, J.; Kästle, G. A.; Emley, N.; Shibauchi, T.; Krusin-Elbaum, L.; Guarini, K.; Black, C. T.; Tuominen, M. T.; Russell, T. P. Ultrahigh-density nanowire arrays grown in self-assembled diblock copolymer templates. *Science* **2000**, *290* (5499), 2126-2129.
2. Ivanov, Y. P.; Chuvilin, A.; Lopatin, S.; Kosel, J. Modulated magnetic nanowires for controlling domain wall motion: toward 3D magnetic memories. *ACS nano* **2016**, *10* (5), 5326-5332.

3. Ivanov, Y. P.; Chuvilin, A.; Vivas, L. G.; Kosel, J.; Chubykalo-Fesenko, O.; Vázquez, M. Single crystalline cylindrical nanowires–toward dense 3D arrays of magnetic vortices. *Scientific reports* **2016**, *6*, 23844.
4. Piraux, L.; George, J. M.; Despres, J. F.; Leroy, C.; Ferain, E.; Legras, R.; Ounadjela, K.; Fert, A. Giant magnetoresistance in magnetic multilayered nanowires. *Applied Physics Letters* **1994**, *65* (19), 2484-2486.
5. Hossain, M. I.; Maksud, M.; Palapati, N. K. R.; Subramanian, A.; Atulasimha, J.; Bandyopadhyay, S. Super-giant magnetoresistance at room-temperature in copper nanowires due to magnetic field modulation of potential barrier heights at nanowire-contact interfaces. *Nanotechnology* **2016**, *27* (30), 30LT02.
6. Yao, J.; Liu, Z.; Liu, Y.; Wang, Y.; Sun, C.; Bartal, G.; Stacy, A. M.; Zhang, X. Optical negative refraction in bulk metamaterials of nanowires. *Science* **2008**, *321* (5891), 930-930.
7. Tsai, K. T.; Wurtz, G. A.; Chu, J. Y.; Cheng, T. Y.; Wang, H. H.; Krasavin, A. V.; He, J. H.; Wells, B. M.; Podolskiy, V. A.; Wang, J. K.; Wang, Y. L.; Zayats, A. V. Looking into meta-atoms of plasmonic nanowire metamaterial. *Nano letters* **2014**, *14* (9), 4971-4976.
8. Chandrasekar, R.; Wang, Z.; Meng, X.; Azzam, S. I.; Shalaginov, M. Y.; Lagutchev, A.; Kim, Y. L.; Wei, A.; Kildishev, A. V.; Boltasseva, A.; Shalaev, V. M. Lasing action with gold nanorod hyperbolic metamaterials. *ACS Photonics* **2017**, *4* (3), 674-680.
9. Zhang, G.; Kirk, B.; Jauregui, L. A.; Yang, H.; Xu, X.; Chen, Y. P.; Wu, Y. Rational synthesis of ultrathin n-type Bi2Te3 nanowires with enhanced thermoelectric properties. *Nano letters* **2012**, *12* (1), 56-60.
10. Gomes, T. D. C. S. C.; Araujo, F. A.; Piraux, L. Making flexible spin caloritronic devices with interconnected nanowire networks. *Science advances* **2019**, *5* (3), eaav2782.

11. Ishihara, S.; Azzarelli, J. M.; Krikorian, M.; Swager, T. M. Ultratrace detection of toxic chemicals: Triggered disassembly of supramolecular nanotube wrappers. *Journal of the American Chemical Society* **2016**, *138* (26), 8221-8227.
12. Muratova, I. S.; Mikhelson, K. N.; Ermolenko, Y. E.; Offenhäusser, A.; Mourzina, Y. Chemiresistors based on ultrathin gold nanowires for sensing halides, pyridine and dopamine. *Sensors and Actuators B: Chemical* **2016**, *232*, 420-427.
13. Sannicolo, T.; Lagrange, M.; Cabos, A.; Celle, C.; Simonato, J. P.; Bellet, D. Metallic nanowire-based transparent electrodes for next generation flexible devices: a Review. *Small* **2016**, *12* (44), 6052-6075.
14. Huang, Q.; Lilley, C. M.; Bode, M. Surface scattering effect on the electrical resistivity of single crystalline silver nanowires self-assembled on vicinal Si (001). *Applied Physics Letters* **2009**, *95* (10), 103112.
15. Vazquez-Mena, O.; Villanueva, G.; Savu, V.; Sidler, K.; Van Den Boogaart, M. A. F.; Brugger, J. Metallic nanowires by full wafer stencil lithography. *Nano Letters* **2008**, *8* (11), 3675-3682.
16. Gu, W.; Choi, H.; Kim, K. Universal approach to accurate resistivity measurement for a single nanowire: Theory and application. *Applied physics letters* **2006**, *89* (25), 253102.
17. Binnig, G.; Quate, C. F. Gerber Ch Atomic force microscope. *Phys. Rev. Lett* **1986**, *56* (9), 930.
18. Rugar, D.; Hansma, P. Atomic force microscopy. *Physics today* **1990**, *43* (10), 23-30.
19. Eaton, P.; West, P. *Atomic force microscopy,* Oxford university press, 2010.
20. Schäfer, S.; Wang, Z.; Zierold, R.; Kipp, T.; Mews, A. Laser-induced charge separation in CdSe nanowires. *Nano letters* **2011**, *11* (7), 2672-2677.
21. Nunes, D.; Calmeiro, T. R.; Nandy, S.; Pinto, J. V.; Pimentel, A.; Barquinha, P.; Carvalho, P. A.; Walmsley, J. C., Fortunato, E.; Martins, R. Charging effects and surface potential variations of

Cu-based nanowires. *Thin Solid Films* **2016**, *601*, 45-53.

22. Zhang, Y. Study of Schottky contact between Au and NiO nanowire by conductive atomic force microscopy (C-AFM): The case of surface states. *Physica E: Low-dimensional Systems and Nanostructures* **2015**, *69*, 109-114.
23. Gramse, G.; Kasper, M.; Fumagalli, L.; Gomila, G.; Hinterdorfer, P.; Kienberger, F. Calibrated complex impedance and permittivity measurements with scanning microwave microscopy. *Nanotechnology* **2014**, *25* (14), 145703.
24. Wu, X.; Hao, Z.; Wu, D.; Zheng, L.; Jiang, Z.; Ganesan, V.; Wang, Y.; Lai, K. Quantitative measurements of nanoscale permittivity and conductivity using tuning-fork-based microwave impedance microscopy. *Review of Scientific Instruments* **2018**, *89* (4), 043704.
25. Ju, Y.; Hamada, M.; Kobayashi, T.; Soyama, H. A microwave probe nanostructure for atomic force microscopy. *Microsystem technologies* **2009**, *15* (8), 1195-1199.
26. Hosoi, A.; Hamada, M.; Fujimoto, A.; Ju, Y. Properties of M-AFM probe affected by nanostructural metal coatings. *Microsystem technologies* **2010**, *16* (7), 1233-1237.
27. Zhang, L.; Ju, Y.; Hosoi, A.; Fujimoto, A. Microwave atomic force microscopy imaging for nanometer-scale electrical property characterization. *Review of Scientific Instruments* **2010**, *81* (12), 123708.
28. Zhang, L.; Ju, Y.; Hosoi, A.; Fujimoto, A. Microwave atomic force microscopy: quantitative measurement and characterization of electrical properties on the nanometer scale. *Applied Physics Express* **2011**, *5* (1), 016602.
29. Feynman, R. P.; Leighton, R. B.; Sands, M. *The Feynman Lectures on Physics: Mainly Electromagnetism and Matter*, 2 Addison, 1977.
30. Pozar, D. M. *Microwave Engineering* 2nd, published by Johnson Wiley and Sons, 1998.

31. Serway, R. A.; Jewett, J. W. *Principles of physics* (Vol. 1). Fort Worth, TX: Saunders College Pub, 1998.

32. Matula, R. A. Electrical resistivity of copper, gold, palladium, and silver. *Journal of Physical and Chemical Reference Data* **1979**, *8* (4), 1147-1298.

Figures

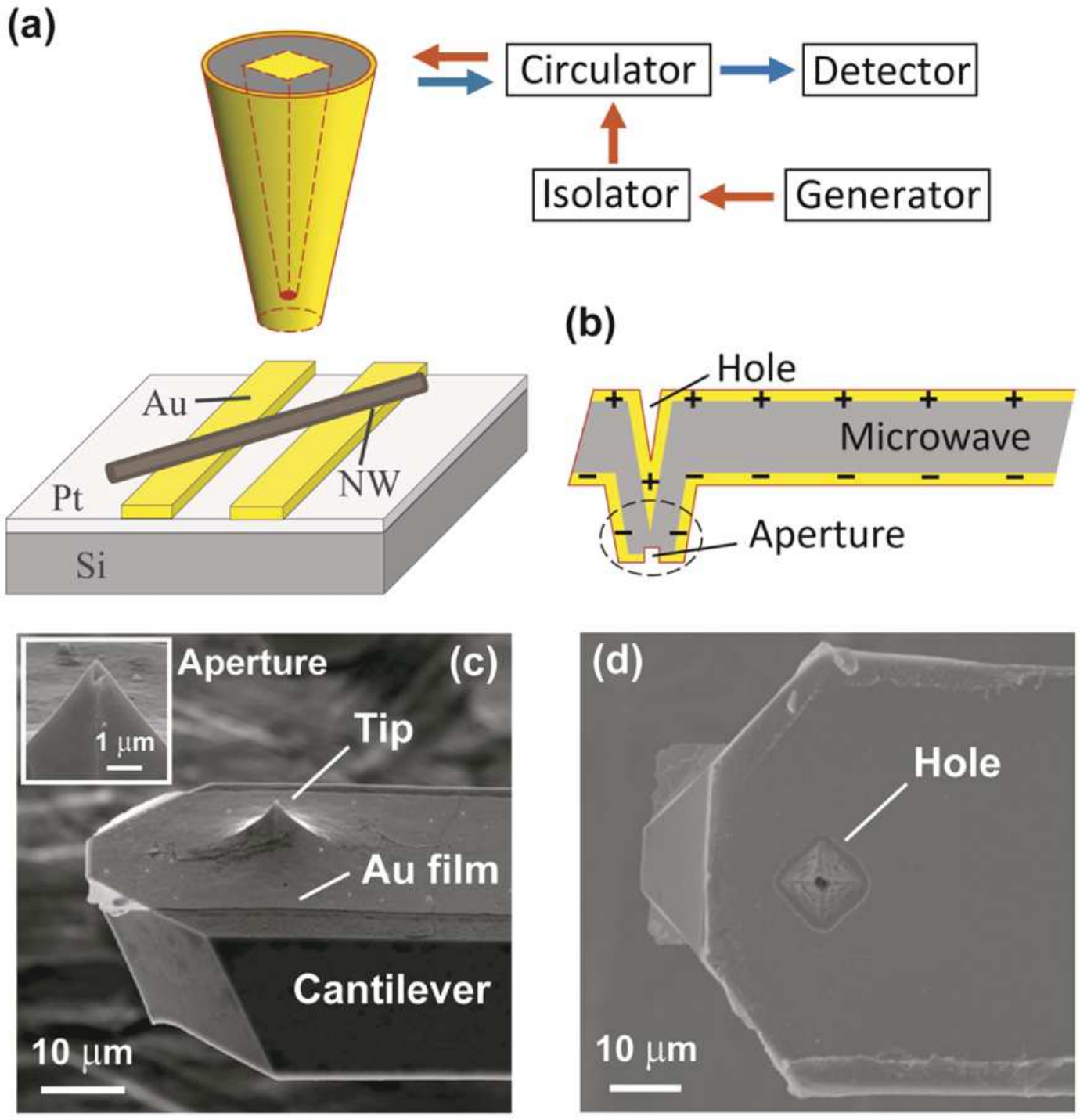

Figure 1

(a) Schematic of the tip of the coaxial M-AFM probe, calibration substrate, and the microwave system. The red arrows indicate the incident signal, and the blue arrows represent the reflected signal. (b) Schematic profile of the coaxial M-AFM probe. The gray and golden parts represent the GaAs and Au films, respectively. The tip in (a) corresponds to the part marked by the dashed circle in (b). SEM images

of the (c) tip side and (d) back side of a coaxial M-AFM probe. The inset in figure (c) depicts the aperture fabricated on the tip.

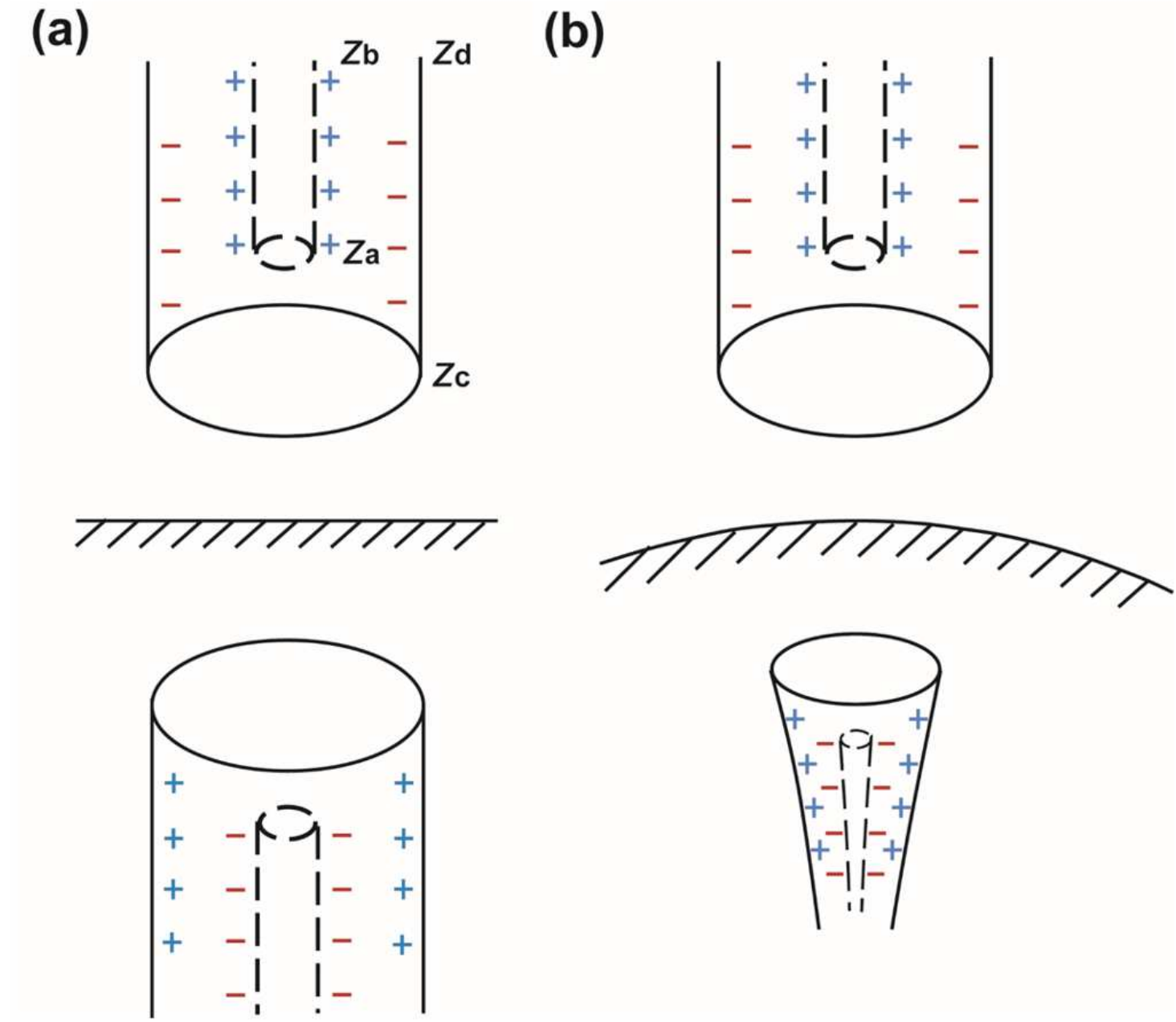

Figure 2

Schematic of image charge when the coaxial probe is over (a) a plane surface and (b) a spherical surface.

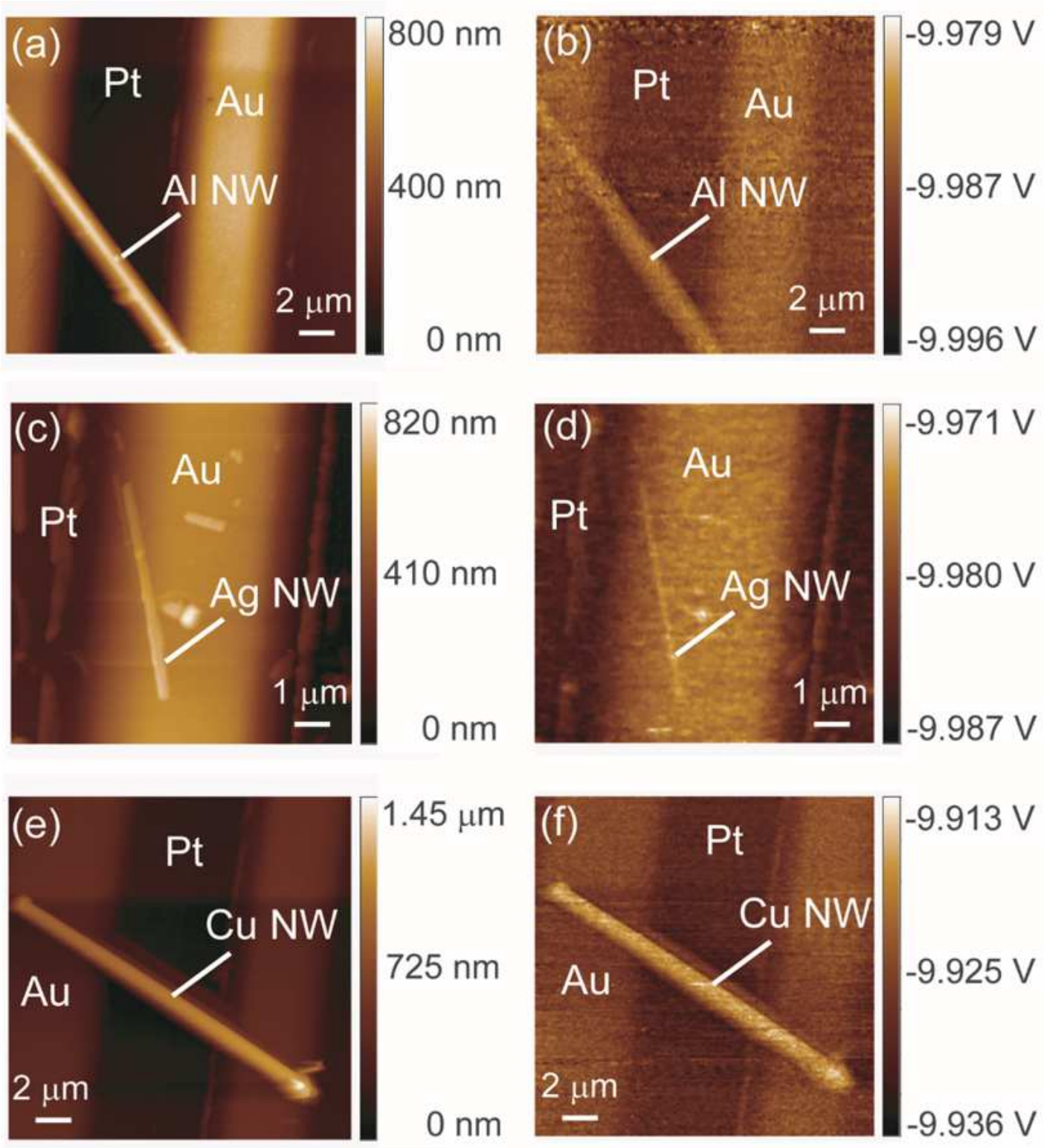

Figure 3

Scanning topography image (left) and microwave signal image (right) of the Al (a, b), Ag (c, d), and Cu (e, f) nanowires on the Pt substrate with Au strips.

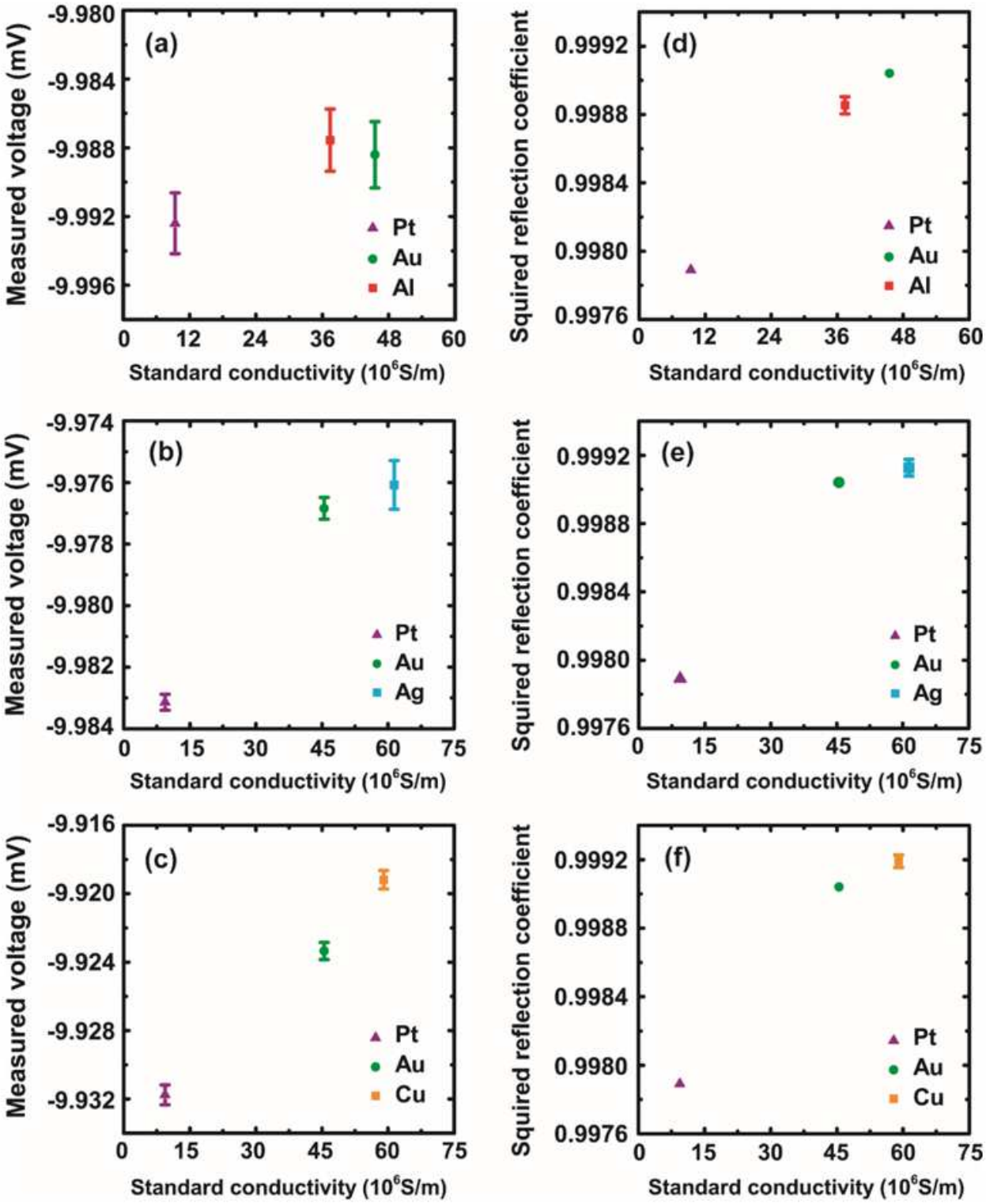

Figure 4

Reflected voltage signals of the (a) Al, (b) Ag, and (c) Cu nanowire samples with the signals of the Pt substrate and Au strip in each measurement, with respect to their standard conductivities. Evaluated results of the square of the surface reflection coefficient |Γ|^2 of the (d) Al, (e) Ag, and (f) Cu nanowire samples with respect to their standard conductivities compared with the theoretical |Γ|^2 values of Au and Pt.

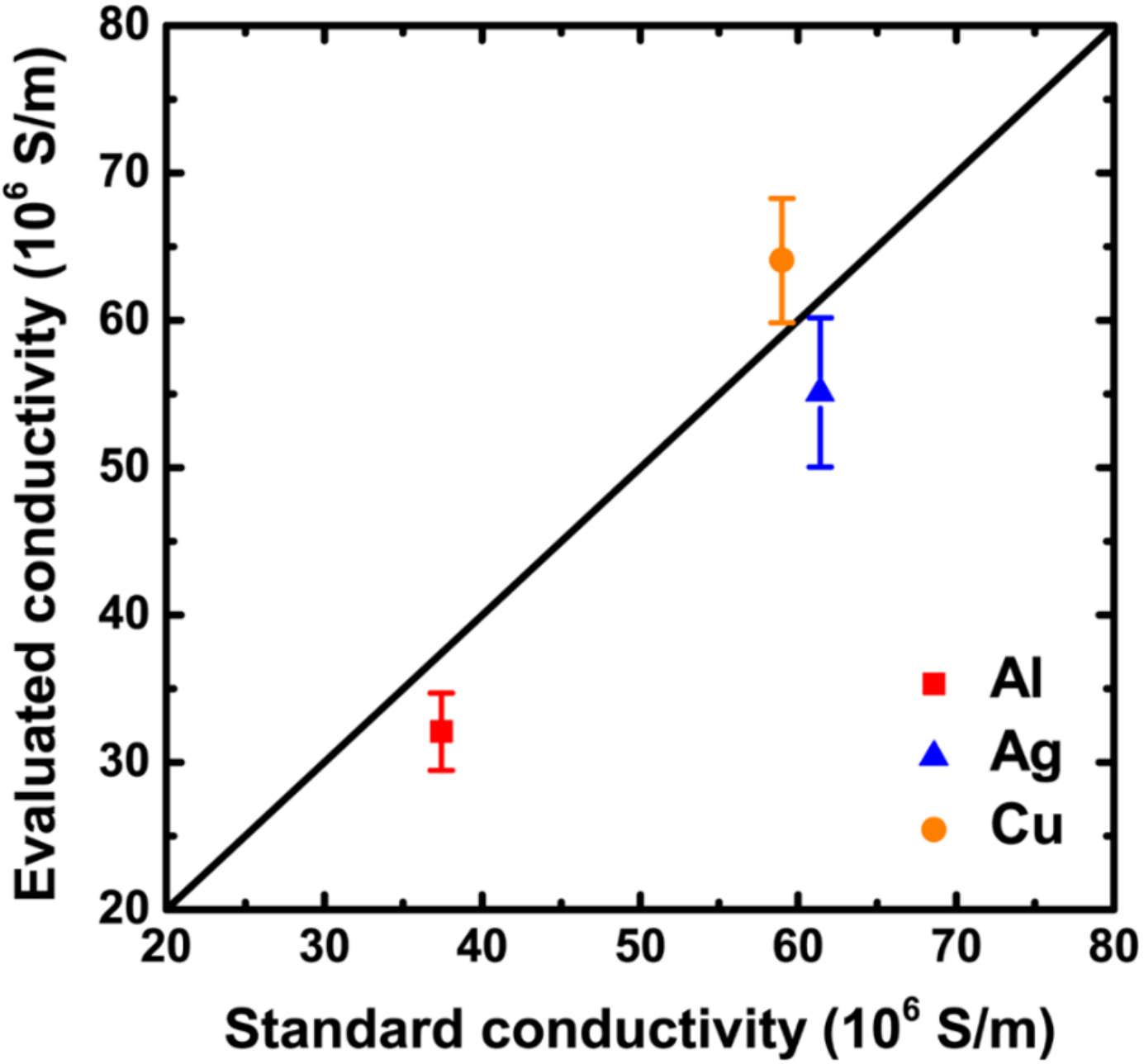

Figure 5

Evaluated conductivities of the Al, Ag, and Cu nanowires compared with their standard values.